Optical Engineering

OpticalEngineering.SPIEDigitalLibrary.org

Phase sensitive distributed vibration sensing based on ultraweak fiber Bragg grating array using double-pulse

Tao Liu
Feng Wang
Xuping Zhang
Lin Zhang
Quan Yuan
Yu Liu
Zhijun Yan

SPIE.

Tao Liu, Feng Wang, Xuping Zhang, Lin Zhang, Quan Yuan, Yu Liu, Zhijun Yan, "Phase sensitive distributed vibration sensing based on ultraweak fiber Bragg grating array using double-pulse," *Opt. Eng.* **56**(8), 084104 (2017), doi: 10.1117/1.OE.56.8.084104.

Phase sensitive distributed vibration sensing based on ultraweak fiber Bragg grating array using double-pulse

Tao Liu,[a] Feng Wang,[a,*] Xuping Zhang,[a,b] Lin Zhang,[c] Quan Yuan,[a] Yu Liu,[a] and Zhijun Yan[d]
[a]Nanjing University, Institute of Optical Communication Engineering, College of Engineering and Applied Sciences, Nanjing, China
[b]Nanjing University, Key Laboratory of Modern Acoustics, Nanjing, China
[c]Aston University, Aston Institute of Photonic Technologies, Birmingham, United Kingdom
[d]Huazhong University of Science and Technology, School of Optical and Electronic Information, Wuhan, China

Abstract. A distributed vibration sensing technique using double-optical-pulse based on phase-sensitive optical time-domain reflectometry (Φ-OTDR) and an ultraweak fiber Bragg grating (UWFBG) array is proposed for the first time. The single-mode sensing fiber is integrated with the UWFBG array that has uniform spatial interval and ultraweak reflectivity. The relatively high reflectivity of the UWFBG, compared with the Rayleigh scattering, gains a high signal-to-noise ratio for the signal, which can make the system achieve the maximum detectable frequency limited by the round-trip time of the probe pulse in fiber. A corresponding experimental Φ-OTDR system with a 4.5 km sensing fiber integrated with the UWFBG array was setup for the evaluation of the system performance. Distributed vibration sensing is successfully realized with spatial resolution of 50 m. The sensing range of the vibration frequency can cover from 3 Hz to 9 kHz. [DOI: 10.1117/1.OE.56.8.084104]

Keywords: optical time-domain reflectometry; optical fiber sensors; ultraweak fiber Bragg grating; vibration measurement.

Paper 170558 received Apr. 13, 2017; accepted for publication Jul. 27, 2017; published online Aug. 19, 2017.

1 Introduction

Vibration sensing is an important application for distributed optical fiber sensors (DOFSs). Among the many DOFSs, phase-sensitive optical time-domain reflectometry (Φ-OTDR) is a very attractive one with the abilities of high sensitivity to vibration, distributed measurement, long sensing range, and so on.[1–4] The basic configuration of a Φ-OTDR sensing system is similar to OTDR but utilizes a very narrow linewidth laser source for the sensing purpose. Thus, the Rayleigh backscattering (RBS) lightwave generated by the forward propagating probe pulse would experience a coherent superposition and exhibit a "jagged" appearance due to the random intensity and phase relationships for the RBS generated from different positions of the fiber. An external disturbance on the fiber can induce the "jagged" signal to have a change at the corresponding position. So the external disturbance can be detected by observing the variation of the signal and its frequency can be obtained by analyzing the frequency spectrum of the signal.

Much research focusing on the performance enhancement of Φ-OTDR have achieved good results, such as enhancing the sensing distance,[5] quantitative measuring the amplitude of vibration with a statistics calculating method[6] and with dual-pulse,[7,8] and improving the detectable frequency range.[9]

However, the RBS coefficient in a fiber is very small. So, normally one has to average many Φ-OTDR curves obtained in different probe pulses to improve the signal-to-noise ratio (SNR).[10] This procedure, however, will decrease the maximum detectable frequency of Φ-OTDR by a factor of N, which is the average number.

The ultraweak fiber Bragg grating (UWFBG) array is a recently developed technique. All the UWFBGs in fiber have the same central wavelength and the same weak reflectivity. When a probe pulse transmits in fiber, only a very tiny portion of the lightwave is reflected by each UWFBG. Thus, the probe pulse can transmit very long distance in the fiber. A few of its applications have been reported for multipoints and distributed sensing purposes.[11–15] Among the research of the UWFBG array assisted Φ-OTDR, Manuel et al.[16] have proposed a semi-UWFBG array to detect the vibration of fiber. In this work, several UWFBG pairs, each of which forms a Fabry–Perot interferometer, are integrated into a fiber. Modulated CW lightwave is used as probe light to extract the information of vibration. The locating algorithm is complicated and multiple simultaneous vibrations having the same frequency cannot be detected. Wang et al.[17] have proposed a fully UWFBG array with a short single probe optical pulse, which needs an unbalanced interferometer to demodulate the signal. Zhu et al.[15] have proposed a distributed Φ-OTDR system with long single probe pulse. However, the pulse width should be at least two times longer than the spatial interval of two adjacent UWFBGs. When the spatial interval is large, the peak power of the optical pulse is severely limited to avoid the nonlinear effect in fiber. And more RBS is generated from an unnecessary part of the probe pulse, which will deteriorate the SNR.

In this paper, we propose a Φ-OTDR system that has the distributed measurement ability with high-frequency response using double-probe-pulse in a sensing fiber integrated with an UWFBG array. Unlike the traditional optical fiber sensor based on the FBG array, which is sensitive only to the events occurring on the position of FBG, the proposed technique is sensitive to the events on any position of the fiber, though it can locate the event only with a spatial

*Address all correspondence to: Feng Wang, E-mail: wangfeng@nju.edu.cn

0091-3286/2017/$25.00 © 2017 SPIE

resolution determined by the spatial interval between two adjacent UWFBGs. By using a double-probe-pulse, a very simple detection setup is enough for receiving the optical signal and locating the events. RBS generated from the useless part of a single probe pulse is eliminated. Very long sensing distance and high-frequency measurement are possible with the proposed technique.

2 Principle

The principle of this technique is shown in Fig. 1. The sensing fiber is integrated with an identical UWFBG array that has a uniform spatial interval. A double-pulse is used as the probe pulse. The spatial interval between the two pulses equals two times the spatial interval of adjacent UWFBGs. When the probe pulse transmits forward in the sensing fiber, the reflected signals of the two pulses from adjacent UWFBGs will overlap and transmit backward together. Because the coherence length of the lightwave is much longer than the spatial interval of the double-probe-pulse, the reflected optical signals will interfere with each other. Apparently, such a probe pulse can make the optical pulse have high peak power to increase the SNR without inducing the nonlinear effect, and the interval of the probe pulse can be adjusted easily to adapt any UWFBG array with uniform interval.

Since the interference occurs between two reflected signals, which may have different powers and polarization states, we use the Jones representation to describe the interference of the two signals. The electric fields of the two signals can be represented as

$$\mathbf{E_1} = A_1 \exp[-i(\omega t + \phi_1)] \quad \mathbf{E_2} = A_2 \exp[-i(\omega t + \phi_2)], \tag{1}$$

where A_n ($n = 1$ or 2) is the amplitude of the reflected signal, ω is the angular frequency of the lightwave, and ϕ_n ($n = 1$ or 2) is the initial phase of the two reflected signals.

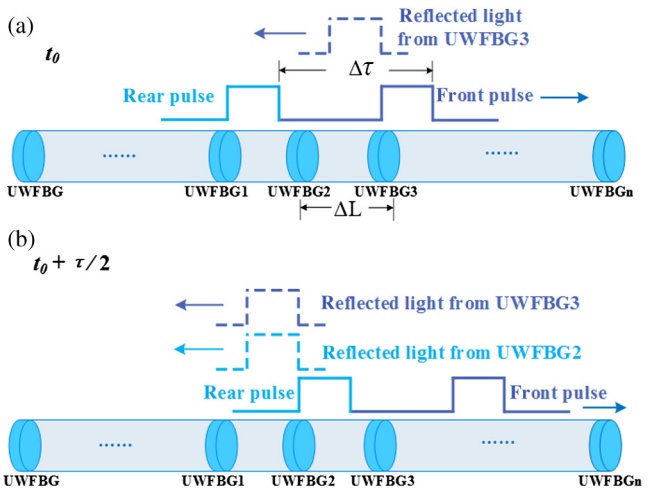

Fig. 1 The process of the generation of the optical signal. (a) The probe pulse is a double-pulse and the sensing fiber is integrated with UWFBG array. (b) The signals reflected by two adjacent UWFBGs overlap and transmit backward together after $\tau/2$, where τ is the time interval between the two pulses.

So the intensity of the coherent signal is

$$\begin{aligned} I &= (\mathbf{E_1} + \mathbf{E_2})^{\dagger}(\mathbf{E_1} + \mathbf{E_2}) \\ &= A_1^2 + A_2^2 + 2A_1A_2\cos(\phi_1 - \phi_2) \\ &= A_1^2 + A_2^2 + 2A_1A_2\cos\delta\phi, \end{aligned} \tag{2}$$

where the note † means the complex transpose.

When the fiber between the two adjacent UWFBGs is disturbed by a vibration, the phase difference $\delta\phi$ of the two signals will change accordingly, which induces the variation of the intensity of the interference. So the disturbance of the fiber can be detected by detecting the intensity variation of the coherent signal.

Since the time interval τ between the two pulses equals to $2n\Delta L/c$, where n is the effective refractive index of the fiber and c is the velocity of light in vacuum, the two pulses will experience different vibration states when they pass the disturbance position successively, which will induce an additional phase difference $\Delta\varphi$. Moreover, the value of $\Delta\varphi$ changes when the probe pulse is injected into the fiber at a different time, because the modulation of a vibration to the optical path is nonlinear for different vibration stages. The shortest period $T_{\min}$ of the vibration, which has the maximum detectable frequency for a Φ-OTDR to a fiber length of L, is $4nL/c$. Thus, when $T_{\min} \gg \tau$, which yields $2L \gg \Delta L$, the additional phase difference $\Delta\varphi$ is very small, resulting in that the change of $\Delta\varphi$ with different vibration stages can be ignored. So the nonlocal effect induced by the change of $\Delta\varphi$ can be ignored. The condition of $2L \gg \Delta L$ can be fulfilled easily since the on-line UWFBGs writing technique can integrate hundreds of UWFBGs in a fiber.[13]

3 Experiment

In experiments, we manufactured a 4.5 km sensing fiber integrated with UWFBG array that has an equal spatial interval of 50 m. Then, we use the experiment configuration as shown in Fig. 2 to measure multiple vibrations to verify the performance of the sensing system. The linewidth of the laser source is 1 kHz. The output lightwave is modulated to the double-pulse by an acoustic optical modulator. The pulse width for each pulse in the probe pulse is 300 ns, the peak power is 8 dBm, and the time interval between the two pulses is 500 ns. The probe pulse is launched into the sensing fiber through a circulator, and the reflected signal is redirected into an avalanche photo diode (APD). A data acquisition card (DAQ) with a sampling rate of

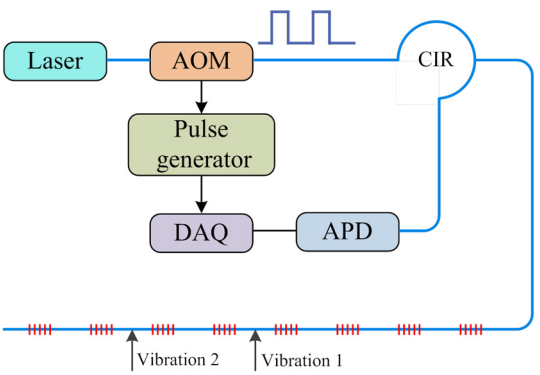

Fig. 2 The experiment setup.

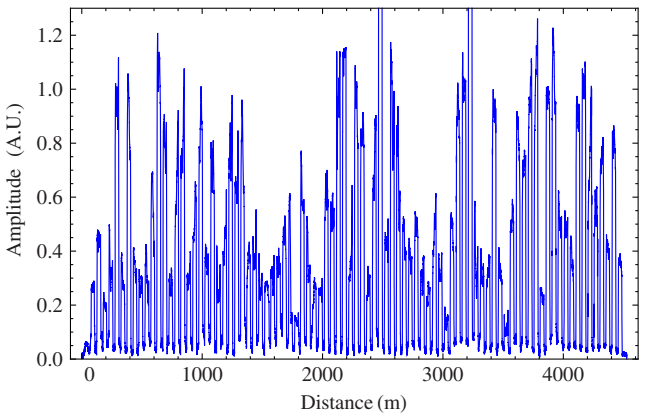

Fig. 3 The obtained coherent signal.

100 MSa/s (corresponding to 10 ns sampling interval) is used to convert the APD signal into digital form and send them to a computer for further processing. Two PZT vibration sources are set at 3.93 and 3.98 km, respectively.

The obtained Φ-OTDR curve is shown in Fig. 3. Since there are 88 integrated UWFBGs in the fiber, there are 89 clear reflective peaks in the curve. The first and the last peaks are induced by the front pulse and rear pulse independently from the first UWFBG and the last UWFBG, respectively. The middle 87 peaks are the coherent results of the reflected signal from the double-pulse. So they have irregular amplitudes each of which is sensitive to the vibration of the fiber section between the corresponding UWFBG pair.

The meaning of the distance axis in Fig. 3 is different from that of the traditional Φ-OTDR. Because each of the reflected coherent signals is generated by two adjacent UWFBGs, whose lengths are on the order of millimeter, the signal represents only the states of the fiber section between the corresponding UWFBG pair.

Two measurements were performed to verify the frequency response and the positioning ability of the sensing system. In the first measurement, the frequencies of the two vibration sources were both at 9 kHz. The repetition time of the probe pulse was 50 μs and the signals for the first 4.5 km were stored for each probe pulse. After acquiring the signals for 0.1 s, 2000 OTDR-curves were obtained. By using the fast Fourier transform method to extract the frequency spectrum of the signals for each position of fiber as Ref. 18, the frequency for each position was obtained. The frequency spectrum along the sensing fiber is shown in Figs. 4(a) and 4(b). Two peaks, both with a frequency of 9 kHz and locating at 3.95 and 4 km, respectively, can be easily observed, which is inconsistent with the experiment condition. The temporal signal at 3.96 km is shown in Fig. 5, where we can see that the frequency of the signal nearly reaches to the limitation of the sampling rate.

In the second measurement, the frequencies of the two vibration sources were set at 3 and 30 Hz, respectively, and the repetition time of the probe pulse was at 500 μs. The frequency spectrum along the sensing fiber is shown in Figs. 4(c) and 4(d), which is derived with 4000 OTDR curves acquired in 2 s. It can be seen that both the 3 and 30 Hz vibrations are detected and positioned in the right positions.

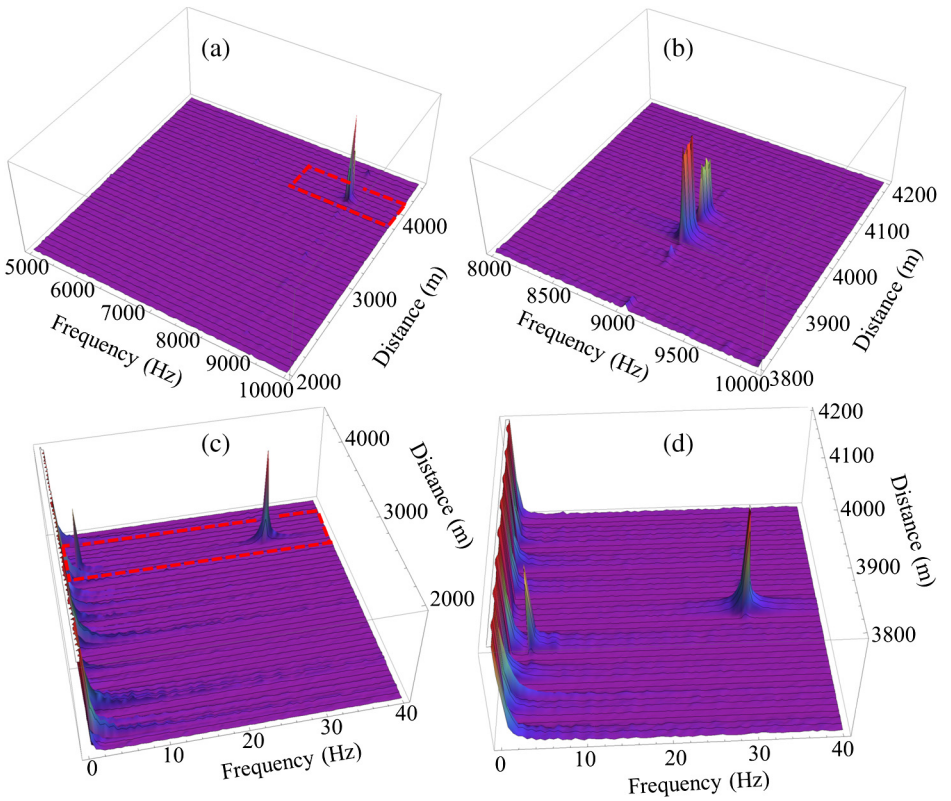

Fig. 4 The distribution of the frequency spectrum along the sensing fiber for (a) two vibrations both with frequencies of 9 kHz and (c) two vibrations with frequencies of 3 and 30 Hz, respectively. (b) and (d) are the enlarged pictures of the dashed areas in (a) and (c), respectively.

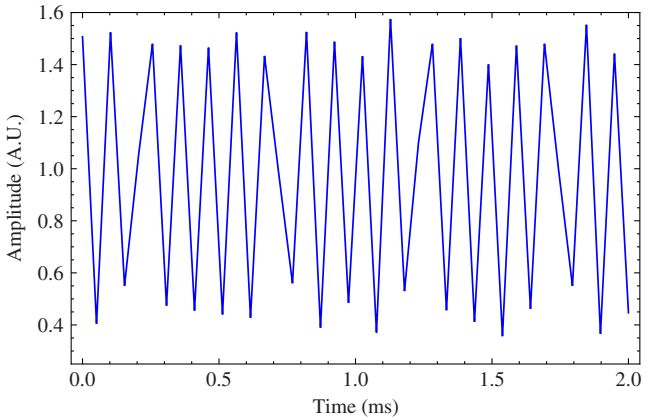

Fig. 5 The temporal signals at 3.96 km in the first measurement.

The reflectivity of the UWFBG is about −40 dB. So the power of the reflected signal for a probe pulse with 300 ns pulse width is about 18 dB higher than that of the RBS. Taking advantage of high SNR, the results were obtained without averaging in both measurements. So the frequency response of the system can almost reach the maximum, which is limited only by the length of fiber.

From Fig. 4(d), it can be seen that there is a very low-frequency component near 0 Hz. This is mainly induced by the low-frequency noise, such as the frequency drifting of the laser source, the temperature fluctuation, and so on, which limits the ability of the system to detect lower frequencies. The suppression of the low-frequency noise will be studied in further research.

4 Discussions

4.1 *Spatial Resolution*

Because the phase difference $\delta\phi$ in Eq. (2) is determined by the state of the whole fiber section between the adjacent UWFBGs, the reflected coherent signal indicates only the summation of all the changes on the whole fiber section. Thus, the spatial resolution of the proposed system is equal to the spatial interval between two adjacent UWFBGs. Since each UWFBG acts like a reflective mirror, the length of the coherent signal for each UWFBG pair equals the pulse width as shown in Fig. 4, and each part of the signal has the same response to the vibration of the fiber in theory. Thus, one can use any part of the signal to demodulate the vibration of the fiber section between the two adjacent UWFBGs. Such a characteristic makes the system more accurate to detect the vibration of the fiber, since many sampling points can provide a collective information to avoid the influence of noise.

4.2 *Signal-to-Noise Ratio of the Signal*

In the proposed system, the received signal representing the $(i-1)$'th and i'th UWFBG pair is composed of three kinds of lightwaves, which are the reflected signals by the two UWFBGs, the multiple reflections between different UWFBGs and the RBS of the probe pulse in the fiber, respectively. The multiple reflections are induced by all the UWFBGs before the current UWFBG pair, thus their summation is influenced by all the fibers before the current position. So the multiple reflections act as noises in the received signal. On the other hand, the RBS is related to the local state of the fiber as a traditional Φ-OTDR. By considering the influence of the RBS, the intensity of the reflected coherent signal is

$$\begin{aligned} I &= (\mathbf{E_1}+\mathbf{E_2}+\mathbf{E_{R1}}+\mathbf{E_{R2}})^{\dagger}(\mathbf{E_1}+\mathbf{E_2}+\mathbf{E_{R1}}+\mathbf{E_{R2}}) \\ &= A_1^2+A_2^2+R_1^2(z)+R_2^2(z)+2A_1A_2\cos\delta\phi \\ &\quad +2A_1R_1(z)\cos[\psi_1(z)-\phi_1]+2A_2R_2(z)\cos[\psi_2(z)-\phi_2] \\ &\quad +2A_1R_2(z)\cos[\psi_2(z)-\phi_1]+2A_2R_1(z)\cos[\psi_1(z) \\ &\quad -\phi_2]+2R_1(z)R_2(z)\cos[\psi_1(z)-\psi_2(z)], \end{aligned} \tag{3}$$

where $R_1(z)$ and $R_2(z)$ are the equivalent amplitude of the coherent RBSs generated by the front and rear pulses, and $\psi_1(z)$ and $\psi_2(z)$ are the equivalent phases of the coherent RBSs.[19] When the double-pulse passes through the vibration position, $\delta\phi$, $\psi_1(z)$, and ϕ_1 vary with the vibration, thus the effective signal can be deduced as

$$\begin{aligned} I_{ac} &\approx 2A_1A_2\cos\delta\phi+2A_1R_2(z)\cos[\psi_2(z)-\phi_1] \\ &\quad +2A_2R_1(z)\cos[\psi_1(z)-\phi_2]. \end{aligned} \tag{4}$$

When the reflected signals and the RBSs are superposed, the summation depends on the relative phase difference between the reflected signals and the RBSs. Because the equivalent phases of the RBSs for different positions are different and even the same vibration of the fiber can induce different coherent RBSs for different positions, the superposition of the reflected signal and the RBSs corresponding to different positions has different responses to the same vibration. Figure 6 shows the signals for different vibration stages around the vibration position for a long single pulse and a double-pulse, respectively. The pulse width of the long single pulse is 800 ns and the pulse width of the double-pulse is 300 ns. Because the interval of two adjacent UWFBGs is 50 m, the long single pulse and the double-pulse have the same length of the overlap section.

From Figs. 6(a) and 6(b), it is very easy to locate the vibration position that is between 1.50 and 1.55 km. However, there are also significant differences between the signals of the long single pulse and the double-pulse. For the long single pulse, the shape of the reflected signal varies obviously for different vibration states and the varying tendencies are different for different positions, whereas for the double-pulse, the shape of the reflected signal approximately remains the same for different vibration stages and thus the varying tendencies are the same for different positions. The difference in the signals is mainly induced by the stronger RBS of the long single pulse. Thus, the RBS may result in different responses to the vibration for different positions. Meanwhile, from Fig. 6(a), one can see that the signal around the overlap section also varies obviously with time, which is because the scattering of the long single pulse superposes with the reflected signal at these positions.

According to Eq. (4), if the adjacent UWFBGs have the same reflectivity and for the ideal case that the reflected signal and the coherent RBSs superpose constructively, the amplitude of the reflected signal is increased by $4\sqrt{P_{\mathrm{ref}}P_{\mathrm{Ray}}}$, where $P_{\mathrm{ref}}=A^2$ is the reflected power from the UWFBG, P_{Ray} is the power of RBS, and we use the expected value

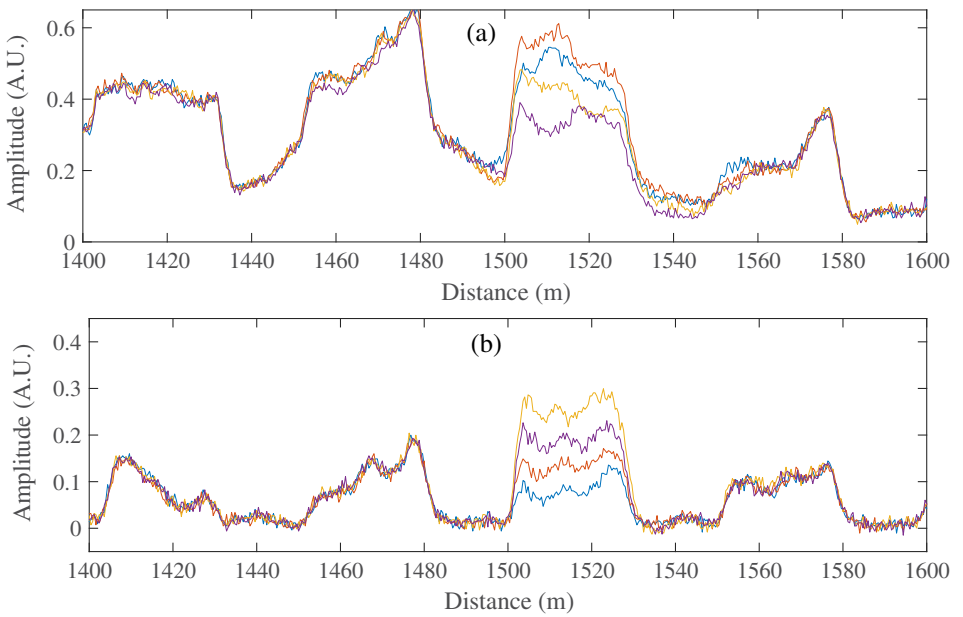

Fig. 6 The signals for different vibration states obtained by (a) a long single pulse and (b) a double-pulse.

of $P_{\mathrm{Ray}} = P_0 S_R v_g \tau$ to represent the equivalent amplitudes $R_1(z)$ and $R_2(z)$ of the coherent RBSs, where P_0 is the peak power of the input lightwave, S_R is the RBS coefficient, v_g is the velocity of lightwave in fiber, and τ is the pulse width of the double-pulse. For a long single pulse, τ can be taken as half of the pulse width for simplicity. Thus, if the pulse width is reduced by a factor of f, the signal enhanced by the RBS will be reduced by $4\sqrt{P_{\mathrm{ref}} P_{\mathrm{Ray}}}(1-\sqrt{1-f})$; however, since the threshold of the nonlinear effect (normally limited by stimulated Brillouin scattering) is increased by a factor of f, the signal can be enhanced by $2fP_{\mathrm{ref}}$ using a stronger optical pulse.[20] Because $S_R = 3.2 \times 10^{-5}$ km^{-1},[21] $v_g \tau$ is less than 100 m, and the reflectivity of the UWFBG is about -40 dB, it is easy to deduce that $2fP_{\mathrm{ref}} \gg 4\sqrt{P_{\mathrm{ref}} P_{\mathrm{Ray}}}(1-\sqrt{1-f})$ for any f. Thus, the preceding analysis indicates that using a double-pulse with short pulse width is better than using a long single pulse.

For the worst case that the reflected signal and the coherent RBSs superpose destructively, the reflected signal has an approximate decrease of $4\sqrt{P_{\mathrm{ref}} P_{\mathrm{Ray}}}$ due to the RBS. Assuming all the UWFBGs have the same reflectivity and neglect the loss of the fiber between adjacent UWFBGs, the SNR of the detected signal under this situation is

$$\mathrm{SNR}(i) = \frac{2P_{\mathrm{ref}}(i) - 4\sqrt{P_{\mathrm{ref}}(i) P_{\mathrm{Ray}}(i)}}{4P_{\mathrm{mul}}(i) + 8\sqrt{P_{\mathrm{ref}}(i) P_{\mathrm{mul}}(i)} + P_{\mathrm{det}}}, \tag{5}$$

where $P_{\mathrm{mul}}(i)$ is the multireflection corresponding to the signal of the i'th UWFBG and P_{det} is the noise-equivalent power (NEP) of the detector.

The generation of the multireflection lightwave has been carefully analyzed in Refs. 13, 15, and 22. By summarizing the conclusions, the elements in Eq. (5) can be given as

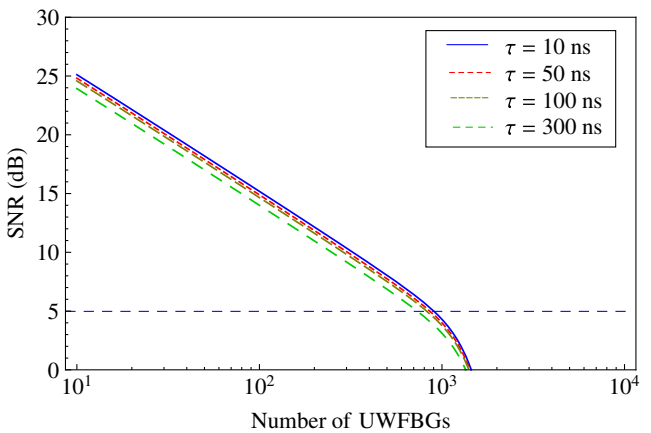

Fig. 7 Simulation result of the SNR evolution with the number of UWFBGs for different pulse widths. The spatial interval between the adjacent UWFBGs is 50 m, the peak power is 100 mW, and the reflectivity of the UWFBG is −40 dB.

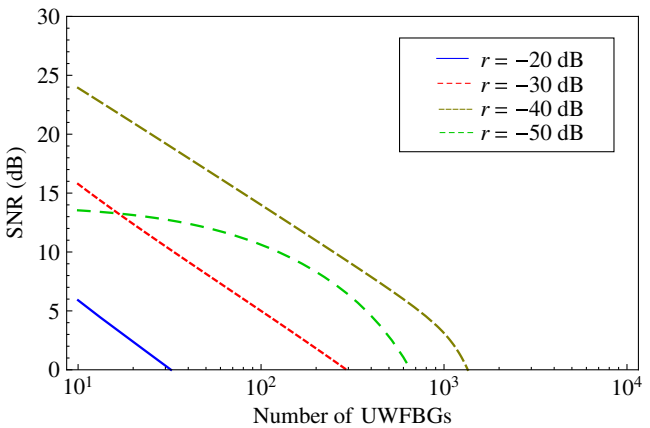

Fig. 8 The SNR evolution with the number of UWFBGs for different reflectivities. The pulse width is 300 ns and the other parameters are the same as that in Fig. 7.

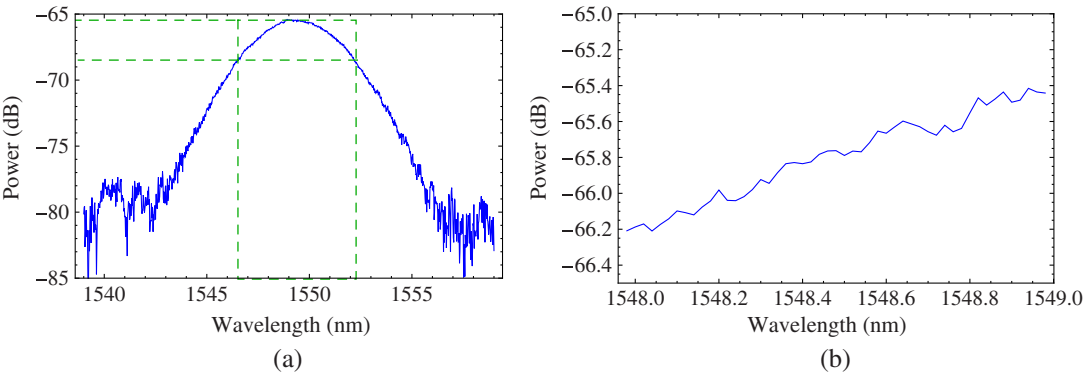

Fig. 9 (a) The reflective spectrum of the UWFBG and (b) the reflective spectrum between 1548 and 1549 nm.

$$\begin{cases} P_{\text{ref}}(i) = P_0 r(1-r)^{2(i-1)} e^{-2\alpha i \Delta L} \\ P_{\text{Ray}}(i) = P_0 (1-r)^{2i} v_g \tau S_{\text{R}} e^{-2\alpha i \Delta L} \\ P_{\text{mul}}(i) = P_0 r^3 (1-r)^{2(i-2)} [(i-1)(i-2)] e^{-2\alpha i \Delta L}/2 \end{cases}, \quad (6)$$

where r is the reflectivity of the UWFBG, $\alpha = 0.046$ km^{-1} is the fiber attenuation coefficient.

Based on Eqs. (5) and (6), two simulations were made to investigate the SNR evolution with the number of the UWFBGs. In the simulations, the NEP of the detector is assumed to be −50 dBm. The first simulation gives the influence of the pulse width to the signal, which is shown in Fig. 7. It can be seen that the SNR decreases with the increment of the pulse width. This is because a longer pulse generates more RBS, and thus has severer impact on the signal. The SNRs for different pulse widths tend to be the same for a long distance, because the power of the probe pulse and the RBS decrease in proportion with the distance, whereas the power of multireflections tends to be constant for a long distance. Figure 7 also shows that the maximum number of the UWFBGs can reach to 900 when the SNR is larger than 5 dB. So the sensing distance for the proposed method can be longer than 45 km.

In the second simulation, the influence of the reflectivity of the UWFBG to the SNR of the system is investigated, which is shown in Fig. 8. It can be seen that a higher reflectivity depletes the power of the probe pulse too soon, which results in a short sensing distance. A very low reflectivity will lead to low SNR and short sensing distance since the RBS dominates in the signal. Therefore, an optimized reflectivity exists for the longest sensing distance. In this simulation, a reflectivity of −40 dB is preferred.

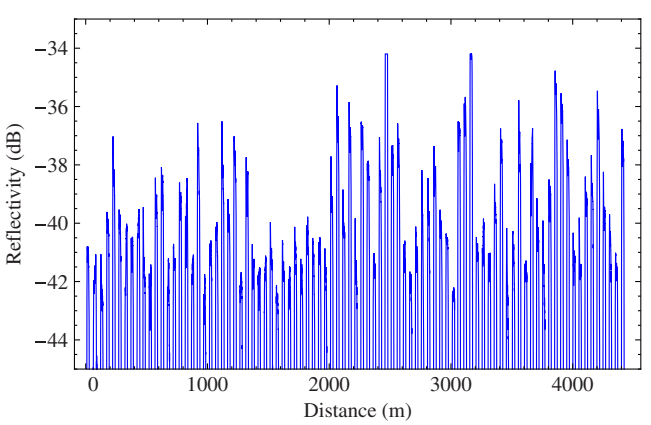

Fig. 10 The reflective relative reflectivities of the UWFBG array.

4.3 *Reflectivity of the Ultraweak FBG*

The length of each UWFBG is about 0.05 mm, which is fabricated by focusing the light spot of a 244 nm UV laser on a phase mask and the bandwidth of the reflective spectrum of the UWFBG is about 5.5 nm, which is shown in Fig. 9. From Fig. 9(b), it can be seen that a 0.2 nm spectral shift, which corresponds to a strain of 175 $\mu\varepsilon$ or a temperature change of 18°C induces a reflectivity change of only 0.24 dB (about 5.7%). Thus, the reflectivity of the UWFBG is very stable to vibration or temperature.

Figure 10 shows the reflected signal of a short single pulse, which can indicate the relative reflectivities of the UWFBG array. By comparing with Fig. 3, it can be seen that some coherent signals are larger, whereas the reflectivity of the corresponding UWFBG is small and vice versa. In Fig. 3, there are even a few signals whose amplitudes exceed the measurement range of the DAQ. We believe it is mainly because of two reasons. One reason is the constructive interference of the reflective signals between the adjacent UWFBGs. The other reason is that the reflectivity of the UWFBG in the corresponding position is too high. Thus, the uniformity of the reflectivities of the UWFBGs should be controlled well in order to get better performance.

5 Conclusion

In conclusion, we propose a Φ-OTDR system that uses double-pulse and sensing fiber integrated with UWFBGs to perform the distributed sensing. The frequency range from 3 Hz to 9 kHz can be realized in a sensing length of 4.5 km. Thanks to the relatively high reflectivity of the UWFBG and long reflected signal from the UWFBG, the measurement can achieve good results without average, so the maximum frequency range is limited only by the fiber length. The system can detect a vibration signal at any position on the fiber and locate the vibration with spatial resolution determined by the spatial interval between the adjacent UWFBGs.

Acknowledgments

This work was supported by the National Natural Science Foundation of China under Grant Nos. 61627816,

61540017, 61405090, and 61307096, and the Fundamental Research Funds for the Central universities under Grant No. 021314380087

References

1. J. C. Juarez et al., "Distributed fiber-optic intrusion sensor system," *J. Lightwave Technol.* **23**(6), 2081–2087 (2005).
2. Q. He et al., "Real distributed vibration sensing with high frequency response based on pulse pair," *Proc. SPIE* **9157**, 915761 (2014).
3. F. Peng et al., "Real-time position and speed monitoring of trains using phase-sensitive OTDR," *IEEE Photonics Technol. Lett.* **26**(20), 2055–2057 (2014).
4. F. Peng et al., "Ultra-long high-sensitivity phi-OTDR for high spatial resolution intrusion detection of pipelines," *Opt. Express* **22**(11), 13804–13810 (2014).
5. Z. N. Wang et al., "Ultra-long phase-sensitive OTDR with hybrid distributed amplification," *Opt. Lett.* **39**(20), 5866–5869 (2014).
6. T. Guojie et al., "The development of an Φ-OTDR system for quantitative vibration measurement," *IEEE Photonics Technol. Lett.* **27**(12), 1349–1352 (2015).
7. A. E. Alekseev et al., "A phase-sensitive optical time-domain reflectometer with dual-pulse diverse frequency probe signal," *Laser Phys.* **25**(6), 065101 (2015).
8. A. E. Alekseev et al., "A phase-sensitive optical time-domain reflectometer with dual-pulse phase modulated probe signal," *Laser Phys.* **24**(11), 115106 (2014).
9. Q. He et al., "All fiber distributed vibration sensing using modulated time-difference pulses," *IEEE Photonics Technol. Lett.* **25**(20), 1955–1957 (2013).
10. Y. Lu et al., "Distributed vibration sensor based on coherent detection of phase-OTDR," *J. Lightwave Technol.* **28**(22), 3243–3249 (2010).
11. Y. Wang et al., "A large serial time-division multiplexed fiber Bragg grating sensor network," *J. Lightwave Technol.* **30**(17), 2751–2756 (2012).
12. X. Li et al., "Simultaneous wavelength and frequency encoded microstructure based quasi-distributed temperature sensor," *Opt. Express* **20**(11), 12076–12084 (2012).
13. H. Chenyuan, W. Hongqiao, and B. Wei, "A novel interrogation system for large scale sensing network with identical ultra-weak fiber Bragg gratings," *J. Lightwave Technol.* **32**(7), 1406–1411 (2014).
14. X. Wang et al., "SNR enhanced distributed vibration fiber sensing system employing polarization-OTDR and ultra-weak FBGs," *IEEE Photonics J.* **7**(1), 680051 (2015).
15. F. Zhu et al., "Improved Φ-OTDR sensing system for high-precision dynamic strain measurement based on ultra-weak fiber Bragg grating array," *J. Lightwave Technol.* **33**(23), 4775–4780 (2015).
16. R. M. Manuel, M. G. Shlyagin, and S. V. Miridonov, "Location of a time-varying disturbance using an array of identical fiber-optic interferometers interrogated by CW DFB laser," *Opt. Express* **16**(25), 20666–20675 (2008).
17. C. Wang et al., "Distributed OTDR-interferometric sensing network with identical ultra-weak fiber Bragg gratings," *Opt. Express* **23**(22), 29038–29046 (2015).
18. L. Zhou et al., "Distributed strain and vibration sensing system based on phase-sensitive OTDR," *IEEE Photonics Technol. Lett.* **27**(17), 1884–1887 (2015).
19. Z. Sha, H. Feng, and Z. Zeng, "Phase demodulation method in phase-sensitive OTDR without coherent detection," *Opt. Express* **25**(5), 4831–4844 (2017).
20. Y. C. Shen et al., "Analysis and measurement of stimulated Brillouin scattering threshold in single mode fiber," *Chin. J. Lasers* **32**(4), 497–500 (2005).
21. D. Derickson, *Fiber Optic Test and Measurement*, pp. 449–454, Prentice Hall PTR, New Jersey (2002).
22. M. Zhang et al., "A large capacity sensing network with identical weak fiber Bragg gratings multiplexing," *Opt. Commun.* **285**(13–14), 3082–3087 (2012).

Biographies for the authors are not available.